Real-time observation of ripple structure formation on a diamond surface under focused ion-beam bombardment

A. Datta, Yuh-Renn Wu,* and Y. L. Wang†

Institute of Atomic and Molecular Sciences, Academia Sinica, P.O. Box 23-166
and Department of Physics, National Taiwan University, Taipei 106, Taiwan

Ripple structures on a diamond surface are created and imaged in real time by focused ion-beam bombardment, and further examined by atomic force microscopy. Beyond a critical incidence angle depending on the ion energy, a ripple structure emerges, and its wavelength remains constant until it breaks down at ~75°. The wavelength is independent of the ion flux, but increases linearly with energy. Addition of a conjectured term representing the redistribution of ion-induced surface species to Makeev, Cuerno, and Barabási's equation allows a quantitative description of the wavelength dependence on the incidence angle.

I. INTRODUCTION

Understanding various morphological evolutions of surfaces created by ion bombardment is of both fundamental and technological interest. One such appealing morphology is the ripple structure formation. Although there is a general consensus about the evolution of ripple structure as being due to competition between surface roughening introduced by sputtering and smoothing created by various processes, all the smoothing mechanisms are yet to be identified. Candidates include pure thermal diffusion,[1–3] viscous flow,[4,5] ion-enhanced or -inhibited diffusion,[6–8] and preferential sputtering without actual mass movement.[9,10] As a result, the exact mechanism for ripple formation remains controversial even twenty years after its first observation. Recently, Makeev, Cuerno, and Barabási (MCB theory)[9,10] generalized Bradley and Harper's second-order linear equation[1] by adding nonlinear and fourth-order terms to address the inadequacies of the theory. The generalized theory introduced an ion-induced smoothing mechanism via preferential sputtering without mass movement on the surface. Being ion induced, the smoothing remains effective when the thermal diffusion is negligible, and therefore makes the wavelength independent of the ion flux at low temperatures. In addition, this theory has many compelling trends including a linear increase of the ripple wavelength with ion energy, and a stabilization of the ripple amplitude at a longer time scale. Although there were some experimental results appearing to indicate the flux independence of the wavelength over a narrow range of fluxes,[11] the presence of a chemical reaction complicates the interpretation of these results. Furthermore, the available experiments[12,13] appear to indicate that, for certain ion-substrate combinations, there exists a minimum incidence angle (the angle between the ion beam and the surface normal) necessary for the formation of a ripple structure. However, there is no such phase-transition-like behavior inherent in MCB theory. For these reasons, a very careful study of ripple formation on a surface with negligible thermal diffusion is warranted. Specifically, the wavelength dependence on the incidence angle and on ion flux needs to be addressed carefully. Therefore, we have used a well-collimated monoenergetic ion beam to create ripple structures on a diamond surface to simplify the comparison between theory and experiment. A diamond surface has negligible surface thermal diffusion at room temperature,[14] and its chemical inertness allows a meaningful comparison between *in situ* and *ex situ* measurements of the ripple wavelength. In order to provide a possible explanation of our experimental results, we propose a mechanism of smoothing due to the slowing down and redistribution of ion-induced surface mobile species. Although ion induced, this mechanism is distinctly different from that proposed by Makeev, Cuerno, and Barabási which does not involve mass movement on the surface. It is also different from ion enhanced or inhibited diffusion[6–8] because it does not involve thermal equilibrium with the surroundings either.

II. EXPERIMENTS

The usual way of creating a ripple structure is to bombard a substrate with a broad ion beam (BIB). In such an experiment, the evolution of the ripple structure is not directly observed, and additional techniques are required for *in situ* study. In comparison to the BIB, the focused ion beam (FIB)[15] has some major advantages for creating and observing ripple structure. It allows *in situ* observation of the formation of ripple structure in real space and time. Furthermore, the FIB is more monoenergetic (energy spread <0.2%) and better collimated (angular spread <1°).[15] These two factors translate, respectively, into better-defined longitudinal and radial straggling of the convoluted profiles of all the collision cascades created by the ions. Such experimental conditions simplify the comparison between experiment and theory.

A 50-KeV Ga FIB system (Micrion 2500) is used to create and observe *in situ* ripple structures of a diamond surface. A contact mode atomic force microscope (AFM) operated in air is used to conduct auxiliary measurement of the topographies of ion-bombarded surfaces. As experimental parameters, the beam energy (5–50 KeV), angle of incidence (0–80°), total fluence (5×10^{16} ion/cm^2 to 1×10^{18} ion/cm^2), and ion flux ($\sim 5 \times 10^{14}$ ion/cm^2 sec to $\sim 10^{19}$ ion/cm^2 sec) are varied. Typically the FIB is scanned over a square area of
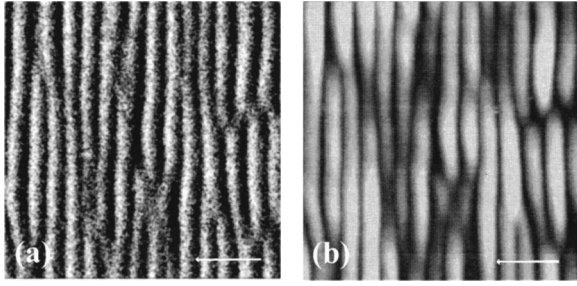
FIG. 1. (a) FIB and (b) AFM images showing the same 2 $\times 2$-μm^2 area (Dose, 1.3×10^{17} ion/cm^2; incidence angle, 55°; beam energy, 50 KeV). The arrow is the direction of the projected ion beam. The amplitude of the ripple is $\sim$10 nm.

4×4 μm^2 by dwelling at each of the 512×512 pixels for a certain amount of time (0.1 μs–1 ms), and scanning over each pixel as many times as required by the desired total dose. Squares as large as 100×100 μm^2 and different-shaped target areas are also created to rule out the effects of boundary. But, except for doses much higher than 10^{19} ion/cm^2, for which the beam incident angle on the boundary area is no longer well defined due to the formation of a deep crater on the bombarded area, no boundary effect is observed. The scanning direction is changed in relation to projected beam direction, and the orientation of the ripple structure is found to be completely independent of the scanning direction. For a beam under the best focusing condition at energy 50 KeV, the beam diameter is $\sim$10 nm. A very small beam current (1.1 pA) is used for such a purpose. The corresponding beam current density (J) is $\sim$1 $\times 10^{19}$ ion/cm^2 sec. The beam current densities are varied by either defocusing the beam and/or by randomly rastering the FIB over different areas using a very short dwell time. The detailed experimental results presented here are from diamond (100) single crystals. However, similar results are observed in experiments performed on other diamond surfaces as well as highly oriented pyrolytic graphite. In conjunction with the fact that high defect density are induced by ion bombardment in the near surface region ($\sim$10 nm) of these structures,[23] we believe that, although the set of results presented here is from diamond (100), the observations are very general in nature for carbon-based materials.

III. RESULTS AND DISCUSSION

In general, real-time observation of ripple structure formation with the FIB provides a tilted view of the target area. The wavelength recorded is then readjusted with the cosine of the tilt angle to obtain the real wavelength. But it is possible to create a ripple pattern with a finite incidence angle, and then record the wavelength with a normal view. Figures 1(a) and 1(b) show the FIB and AFM images of the same area of a typical ripple structure, respectively. The ripple structure and, especially, its wavelength l_x appear essentially the same in the images, demonstrating the capability of the FIB for *in situ* observation.

The amplitude of the evolving ripple structure cannot be obtained either in real time or *in situ* with the current setup
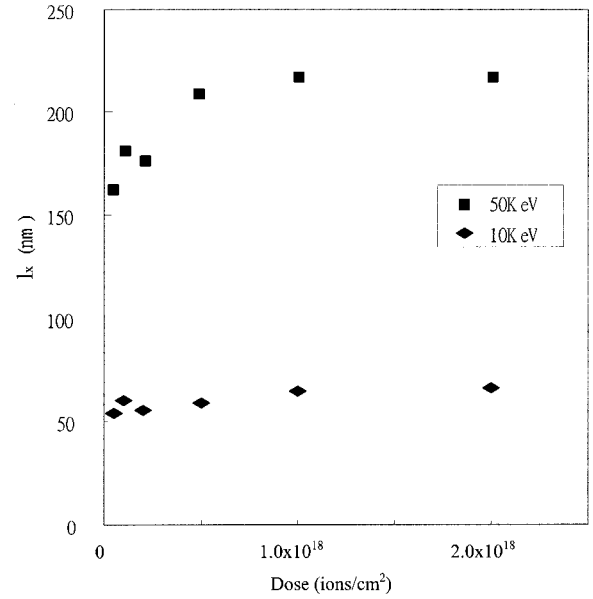

FIG. 2. Variation of the dominant ripple wavelength with ion dose. The energies are 50 and 10 KeV. The ion incidence angle is 60°.

of our FIB. However, *ex situ* AFM study of the amplitude shows a trend very similar to the reported results:[9] it grows quickly initially, and finally saturates at a high dose. The wavelengths reported here are measured from ripples with amplitudes between 2 and 6 nm for 5-keV ions and 7 and 39 nm for 50-keV ions. In these ranges, amplitudes are still growing, but at a reduced rate.

After a matured appearance of the ripple structure, no significant real-time movement of the wave fronts is observed in the direction of the projected ion beam. However, formation, movements, and collapse of different features such as pinching points are observable during ion bombardment, but these do not affect the wavelength directly within our experimental range. It should be noted that the fixed finite boundary in our experiment may have some effects on the propagation of the wave fronts. Caution should be taken when attempting to compare our results with theories in this regard.

Figure 2 shows the variation of the ripple wavelength with the delivered ion dose at energies of 50 and 10 KeV with 60° ion-incidence angle. The average wavelength is measured directly from AFM images as well as from the two-dimensional (2D) Fourier transform of the images. Uncertainty in the measurement is estimated to be $\sim$10%. The ripple wavelength initially grows at a faster rate, and then almost saturates. The wavelengths considered in our later discussions are taken from this semisaturated region.

Figure 3 shows the variation of the average wavelength of the ripple structure with the change of the incident angle for 50 and 10-KeV beam energies. From this result, it is evident that below a critical incidence angle a ripple structure does not appear. Instead, the surface becomes smoother than the starting surface. A decrease in the critical angle by $\sim$10° is observed when the energy is increased from 10 KeV (50°) to 50 KeV (40°). Once the ripple structure appears, its wave-
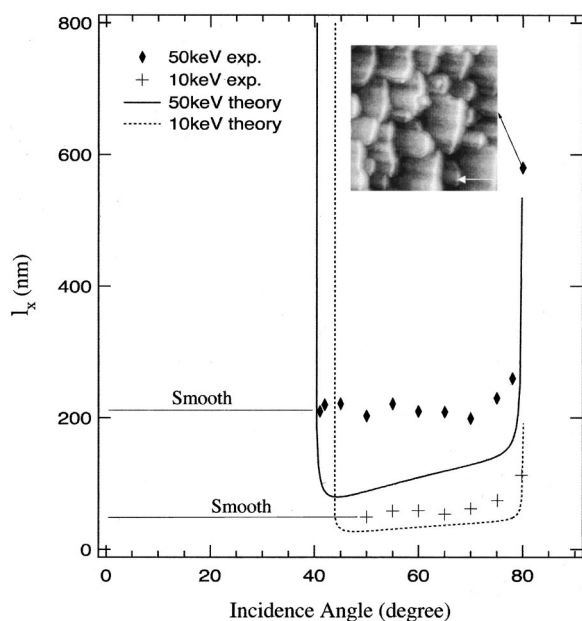
FIG. 3. Variation of the dominant wavelength l_x with incidence angles at 50 and 10 KeV. The inset shows the broken ripple topography at an 80° incidence angle after a dose of 5×10^{17} ion/cm^2 is delivered; the arrow shows the direction of the projected ion beam. The continuous and dotted lines are theoretical fits for 50 and 10-KeV beam energies, respectively.

FIG. 4. A typical variation of root-mean-square roughness vs ion dose. The ions are delivered at an ion-incidence angle 30° onto areas with ripple structures. The continuous line is to guide the eye.

length is not sensitive to a change in angle until 75°. Beyond 75°, the ripple pattern starts to break down, and gives rise to a different morphology, as shown in the inset of Fig. 3. Although from a 2D Fourier transform it is determined that the structure is still predominantly oriented in the x direction (i.e., the ripple wave vector is in the same direction as projected ion-beam direction), structures along the y direction start to appear. As the ripple structure is broken in such a case, defining a wavelength becomes difficult. The dominant length scale starts to increase with the angle at a much higher rate. This second critical angle for a large change in length scale is between 75° to 80° for all the energies studied. Hence the evolving morphology of the diamond surface under ion bombardment can be divided into three distinct categories according to increasing incidence angle, namely, a smooth surface, a surface with well-defined ripple topography, and a surface with broken ripple topography.

The sudden appearance of a ripple structure at particular incidence angles indicates that the chemical nature of the surface does not play much of a role in this phase-transition-like behavior. The reason behind such an argument is that there cannot be a sudden change of chemical composition of the surface due to a small change in the ion incidence angle. There have been arguments and counterarguments in this regard,[11,16] but established facts seem to support this view.[17]

In order to understand the effect of smoothing, ripple structures are created by 50-KeV FIB (the ion dose is 1 $\times 10^{18}$ ion/cm^2) using an ion-incidence angle of 55°, and the structures are further bombarded with the FIB at smaller incidence angles. The ion doses used for smoothing in these areas are increased systematically from 2×10^{17} to 1
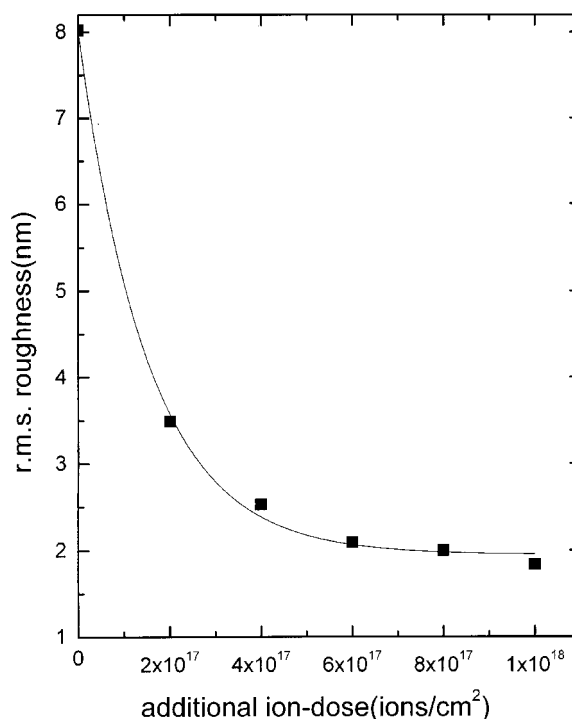
$\times 10^{18}$ ion/cm^2 for each ion-incidence angle. The root-mean-square roughness for the resulting surfaces are measured with an AFM.

Figure 4 provides a typical variation of rms roughness with ion dose at an ion-incidence angle of 30° with a 50-KeV Ga ion beam. The rms roughness decreases exponentially with increasing ion dose. We tested the trend in other ion-incidence angles as well, and the results were similar. All these ion-incidence angles are below the critical limit for the creation of a ripple structure. The initial rms roughness for the pristine diamonds used for this set of experiments are in the range of ~ 3–5 nm. The final roughness achieved after a total dose of 1×10^{18} ion/cm^2 is ~ 1.8 nm. For comparison, a pristine diamond surface is directly bombarded with an ion dose of 1×10^{18} ion/cm^2 at an incidence angle of 30°, and the final rms roughness achieved is ~ 1.1 nm. So, for ion bombardment at ion-incidence angles below the critical angle for the smooth-ripple transition, the surface actually becomes smooth, as stated earlier, no matter whether the starting surface has random roughness or has a regular ripple pattern on it.

Figure 5 shows the variation of wavelength l_x with ion flux for a typical incidence angle (57°). The two insets show ripple structures corresponding to two extreme cases of flux separated by almost five orders of magnitude ($\sim 10^{19}$ to $\sim 5 \times 10^{14}$ ion/cm^2 sec). The energy used is 50 KeV. This clearly demonstrates that the wavelength is independent of the flux of the ion beam for this particular surface at room temperature. Generally for a BIB system, it is difficult to vary the ion flux accurately over a wide range. If there were a weak flux dependence of the wavelength, with a small
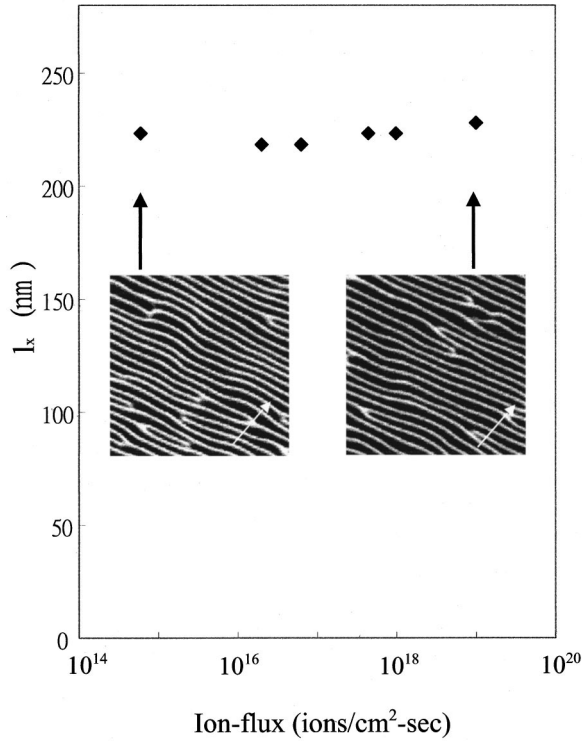
FIG. 5. Variation of dominant wavelength l_x with ion flux (beam energy, 50 KeV; dose, 5×10^{17} ion/cm^2; incidence angle, 57°). The insets show *in situ* FIB images of the ripple structures corresponding to two extreme fluxes. The arrow shows the direction of the projected ion beam.

FIG. 6. Variation of dominant wavelength l_x with beam energy, at doses of 5×10^{17} and 1×10^{18} ion/cm^2.

variation of the ion flux it would be very difficult to determine the change. This result therefore signifies that surface thermal diffusion, which would have introduced flux dependence,[1] is negligibly small. The ion-enhanced or -inhibited surface diffusions, which also introduce flux dependence of wavelength but in different ways,[6–8] are not noticeable either.

Figure 6 shows a variation of the wavelength l_x with energy at two typical ion-incidence angles (45° and 60°). For a particular dose, as long as a ripple structure appears, the wavelength increases linearly with the energy (5–50 KeV), irrespective of incidence angle and flux. This particular trend is consistent with the theoretical framework recently suggested by Makeev, Cuerno, and Barabási,[9,10] but was not addressed in the theory originally proposed by Bradley and Harper.[11]

The feature size, especially ripple wavelength, is found to be independent of the beam spot size. At a particular energy, with defocusing or with a changed beam current density, the wavelength remains constant. With a lowering of energy, the spot size increases but the wavelength becomes increasingly smaller. Actually, the feature size is a direct consequence of the size of the collision cascade, which, at a particular energy, does not change with defocusing or the beam current.

IV. THEORY

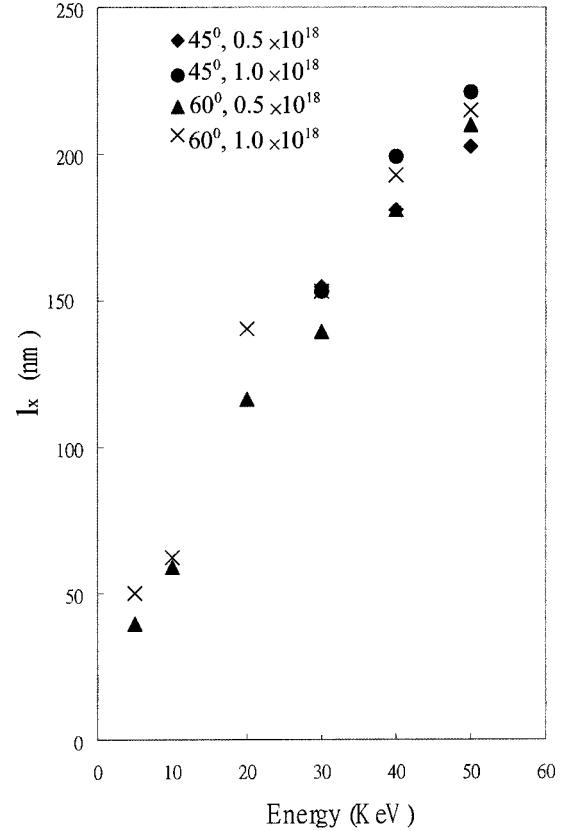The evolving surface topography under ion bombardment can be described by a single-valued height function $h(x,y,t)$, measured from an initial smooth configuration which is taken to lie in the (x,y) plane. The ion beam is taken to be parallel to the x-h plane, forming an angle $0 < \theta < \pi/2$ with the h axis. The time evolution of the surface under the condition of negligible thermal surface diffusion at a smaller time scale, which resembles our experimental situation, can be described by the MCB equation for the linear case with asymmetric straggling:

$$\frac{\partial h}{\partial t} = -V_0 + \gamma \frac{\partial h}{\partial x} + v_x \frac{\partial^2 h}{\partial x^2} + v_y \frac{\partial^2 h}{\partial y^2} - D_x^I \frac{\partial^4 h}{\partial x^4} - D_y^I \frac{\partial^4 h}{\partial y^4},$$

(1)

where V_0 is the average erosion rate. The second term accounts for uniform motion of the surface features along the x direction. Parameters v_x and v_y represent the ion-induced roughening coefficients, and were originally calculated by Bradley and Harper.[1] The value of v_x is negative at a lower incidence angle, and becomes positive at a higher incidence angle, while that of v_y is always negative. The orientation of the ripple structure is determined by the larger magnitude of these coefficients while they are negative. D_x^I and D_y^I are the coefficients of the ion-induced diffusion in the x and y directions. This diffusionlike mechanism originates from preferential sputtering and does not involve actual mass movement. It has been shown by simulation that existence of such mechanism alone can justify stable ripple structure formation.[18] The detailed expressions for the relevant coefficients can be found in Refs. 9 and 10.

The wavelength of the ripple structure under such a circumstance is given by:

$$l_x = 2\pi \left(\frac{2D_x^I}{\nu_x} \right)^{1/2}, \tag{2}$$

which is completely flux independent. Although this trend, and the trend of linear dependence of the wavelength on energy generated by this theory are consistent with our results, this theory does not generate a phase transition from a smooth surface to a ripple surface at a critical incidence angle. At lower incidence angles, as we have mentioned, both ν_x and ν_y are negative. Therefore, Eq. (1) predicts formation of ripple structure under such condition unless some other smoothing effect takes place.

Mathematically, by adding a term $\nu_0 \nabla^2 h$ to this equation, where ν_0 is a positive number proportional to ion flux, will automatically create a smooth-ripple transition while keeping the wavelength independent of the ion flux (J) since both D_x^I and D_y^I as well as ν_x and ν_y, are all proportional to J. Conceptually, this additional term cannot originate from thermal diffusion, with or without the effect of ion bombardment, because adding such a diffusion term $D_0 \nabla^4 h$ to Eq. (1) will lead to a wavelength dependence on the ion flux.[1,6–8]

One of the candidates for such a smoothing mechanism is the movement of surface species induced by ion bombardment through a collision cascade. Experimentally, it was been found that the number of such species is proportional to the ion flux.[19] From a mathematical formulation, it appears that the smoothing effect should be introduced through a nondiffusive process, in order to generate a smooth-ripple transition based on the ion-incidence angle. We find, from a TRIM code calculation,[20] that there is a substantial number of mobile species on the surface, induced by the underlying collision cascade due to each ion impact. Although these mobile species do not have adequate energy to escape from the surface barrier, their mean energy is as high as $\sim$3 eV. It is known that the TRIM code becomes fairly inadequate for simulating the dynamics of low-energy surface atoms. However, the TRIM code can provide the energy distribution of the particles that rise to the surface due to the collision cascade induced by ion impact. The sputtering yield, which is determined by integrating this distribution starting from a cutoff introduced by the surface binding energy, is known to match with the experimental results within a factor of 2 in most cases. It is therefore reasonable to use the TRIM code to roughly estimate the average number of particles that reach the surface without leaving it, by considering the same distribution below the cutoff. Although not as accurate as sputtering yield, this is adequate, at least within an order of magnitude. Even based on this order-of-magnitude calculation, it can be concluded that these mobile species are hyperthermal in nature, as compared to surroundings (room temperature $\sim$0.025 eV) and no thermal equilibrium with the surroundings is expected at least at the beginning of the journey of these hyperthermal mobile species.

Now the question is how a number of hyperthermal mobile species redistribute themselves on an evolving curved surface with a nondiffusive motion. To the best of our knowledge, very little is known about the final distribution for such a hyperthermal situation. We propose a conjecture that species with such high-energy should move quite a long distance on the surface depending on the energy loss per jump, until they are thermalized to background by dissipation of energy. It acts as a random slowing down process through a dissipation of energy. To a first approximation, the final distribution of such hyperthermal species on a macroscopically curved surface can be related to its curvature, as indicated by our preliminary simulation results.[21]

Another proposed candidate for the smoothing term is based on the increasing anisotropy of the recoils as the incidence angle increases.[13] To the best of our knowledge, such anisotropy was never observed experimentally. In addition TRIM code-based calculations also do not generate any significant anisotropy in the momentum distribution of the hyperthermal surface species on this surface with increasing incidence angle.

We therefore propose a modification of the roughening coefficients [ν_x and ν_y in Eq. (1)] as a result of competition between the roughening induced by sputtering and smoothing by the movement of hyperthermal species induced by underlying collision cascade. The two modified roughening coefficients are: $\nu_x' = \nu_x + \nu_0$ and $\nu_y' = \nu_y + \nu_0$ where $\nu_0 = J\gamma Y_m / n^2 \Delta\varepsilon$, with J the ion flux (ion/cm^2 sec); n the density of the target (atoms/cm^3); γ the surface free energy per unit area; Y_m the number of mobile surface atom per incident ion, and $\Delta\varepsilon$ is a constant proportional to the energy loss per unit jump of the mobile atom.

Taking the ion range and lateral and longitudinal stragglings from the TRIM code simulation, and using ν_0 as a fitting parameter for matching the critical angle for the smooth-ripple transition while ignoring its possible dependence on the incidence angle, the theory can be quantitatively compared with our experiments. Surprisingly, with a single $\nu_0 = 1 \times 10^{-19}$ cm^2/s, the theoretical calculation generates a wavelength dependence on the incidence angle that is consistent (within a factor of 2) with the experimental results for both beam energies, as shown in Fig. 2. The theoretical curves also show the correct trend of smaller critical angle necessary for the phase transition associated with larger energy. To our knowledge, this is the closest quantitative comparison between theory and experiment for the wavelength of ripple structure formation by ion bombardment of a surface. Although it is possible to fine tune ν_0 based on specific values of its constituent parameters, depending on ion energy to improve the fitting, we think it is premature at this juncture to do so, as adequate inputs are not available either from theory or experiment. Inputs from the TRIM code simulation are also not accurate enough for terms such as Y_m, as already stated.

In our experiment, we did not see any clear turning of the ripple structure with the increase of the incidence angle up to 80°. Under such a grazing incidence angle, Sigmund's sputtering theory for the creation of microroughening is not valid.[1,22] Also, as the roughening coefficients ν_x' and ν_y' become comparable, ripple structures in other directions also start to form. The rather complex structures observed could be a combined result of all these factors.

V. CONCLUSION

In summary, we have created and observed ripple structures on a diamond surface with a focused ion beam. The structures, which are chemically inert, were further studied using *ex situ* atomic force microscopy. The ripple wavelength is flux independent but linearly dependent on the ion energy within the experimental range. A modified version of the MCB equation with ion-induced hyperthermal mass movement is proposed to explain the smooth-ripple phase transition occurring at a critical ion-incidence angle. This critical angle is found experimentally to shift to a lower value for a higher energy. Such an equation naturally leads to a flux-independent wavelength of the ripple structure, consistent with our experiments. When a ripple structure is bombarded by an ion beam below the critical incident angle, its rms roughness is found to decrease exponentially with increasing dose. Further theoretical efforts are needed to quantitatively address the effects of nonlinearity and white noise terms[10] on the wavelength dependence on the incidence angle.

*Present address: Graduate Institute of Communication Engineering, National Taiwan University, Taipei 106, Taiwan.

†Electronic address: ylwang@po.iams.sinica.edu.tw

[1] R. M. Bradley and J. M. E. Harper, J. Vac. Sci. Technol. A **6**, 2390 (1988).

[2] C. Herring, *Physics of Powder Metallurgy* (McGraw-Hill, New York, 1951), p. 143.

[3] W. W. Mullins, J. Appl. Phys. **28**, 333 (1957).

[4] E. Chason, T. M. Mayer, B. K. Kellerman, D. T. McIlroy, and A. J. Howard, Phys. Rev. Lett. **72**, 3040 (1994).

[5] J. Erlebacher, M. J. Aziz, E. Chason, M. B. Sinclair, and J. A. Floro, Phys. Rev. Lett. **82**, 2330 (1999).

[6] S. W. MacLaren, J. E. Baker, N. L. Finnegan, and C. M. Loxton, J. Vac. Sci. Technol. A **10**, 468 (1992).

[7] S. M. Rossnagel, R. S. Robinson, and H. R. Kaufman, Surf. Sci. **123**, 89 (1982).

[8] R. Ditchfield and E. G. Seebauer, Phys. Rev. Lett. **82**, 1185 (1999).

[9] M. A. Makeev and A.-L. Barabási, Appl. Phys. Lett. **71**, 2800 (1997); M. Makeev, R. Cuerno, and A-L. Barabási, (private communication).

[10] S. Park, B. Kahng, H. Jeong, and A.-L. Barabási, Phys. Rev. Lett. **83**, 3486 (1999).

[11] J. J. Vajo, R. E. Doty, and E.-H. Cirlin, J. Vac. Sci. Technol. A **14**, 2709 (1996).

[12] G. Carter, V. Vishnyakov, and M. J. Nobes, Nucl. Instrum. Methods Phys. Res. B **115**, 440 (1996).

[13] G. Carter and V. Vishnyakov, Phys. Rev. B **54**, 17 647 (1996).

[14] E. A. Eklund, R. Bruinsma, J. Rudnick, and R. S. Williams, Phys. Rev. Lett. **67**, 1759 (1991).

[15] Y. L. Wang and Z. Shao, in *Advances in Electronics and Electron Physics*, edited by P. W. Hawkes (Academic, Boston, 1991), Vol. 81, p. 177, and references therein.

[16] H. Shichi, K. Ohnishi, and S. Nomura, Jpn. J. Appl. Phys., Part 2 **30**, L927 (1991).

[17] M. A. Makeev and A.-L. Barabási, Appl. Phys. Lett. **72**, 906 (1998).

[18] I. Koponen, M. Hautala, and O.-P. Sievänen, Phys. Rev. Lett. **78**, 2612 (1997).

[19] J. Y. Cavaillé and M. Drechsler, Surf. Sci. **75**, 342 (1978).

[20] J. F. Zeigler and J. P. Biersack, SRIM (TRIM 90) Simulation package (1995), IBM Research, 28-024 Yorktown, NY, 10598.

[21] Yuh-Renn Wu (unpublished).

[22] P. Sigmund, J. Mater. Sci. **8**, 1545 (1973).

[23] A. Datta, Yuh-Renn Wu, and Y. L. Wang, Appl. Phys. Lett. **75**, 2677 (1999).